Malaysian Journal of Catalysis
http://mjcat.utm.my/
MJCat
Research Article

Commercial Silica-Supported Niobium-Doped Titanium Dioxide for The Photocatalytic Degradation of Methylene Blue

Nur Nadia Binti Zalirizal[1],Chui Min Ling[1], Nursyafreena Attan[1], *Siew Ling Lee[1,2*,]

[1] *Department of Chemistry, Faculty of Science, Universiti Teknologi Malaysia, 81310 UTM Johor Bahru, Johor, Malaysia*
[2] *Centre for Sustainable Nanomaterials, Ibnu Sina Institute for Scientific and Industrial Research, Universiti Teknologi Malaysia, 81310 Johor Bahru, Johor, Malaysia.*

**Corresponding Author: Tel: +60177165916 (lsling@utm.my)*

Article history :
Received 27 March 2026
Revised 26 May 2026
Accepted 1 June 2026

ABSTRACT

Water contamination from mutagenic dyes has intensified research into Advanced Oxidation Processes (AOPs), a promising method for mineralizing dye pollutants. The widely used TiO_2 catalyst can overcome this issue; however, it still agglomerates despite its high catalytic activity, thereby reducing surface area and increasing charge recombination. To overcome this limitation, this study modified a niobium-doped titania photocatalyst by introducing fumed silica, a high-surface-area support, to improve titania dispersion. A series of SiO_2/Nb-TiO_2 photocatalysts with different silica-to-titania molar ratios was prepared via the sol-gel method with sonicator assistance and characterized by X-ray diffraction (XRD), Fourier transform infrared-attenuated total reflectance (FTIR-ATR), diffuse reflectance UV-Visible spectroscopy (DRUV-Vis), and nitrogen adsorption-desorption analysis. XRD analysis confirmed anatase TiO_2 phase presence, successful substitution of niobium into the titania lattice, and the appearance of a broad amorphous hump in the silica-supported catalyst (20 SiO_2/Nb-TiO_2). DRUV-Vis Spectroscopy revealed that the absorption edge of the silica-supported samples shifted to deeper ultraviolet light due to quantum-size effects. Among all samples, the optimum silica molar ratio was 10 SiO_2/Nb-TiO_2 due to a lower bandgap, the highest surface area (180.81 m^2/g), and the highest degradation activity (76.60%) at a 5 ppm methylene blue. These findings demonstrate the synergistic effects of niobium doping and an optimal silica support on photocatalyst performance.

Keywords: *Fumed silica, Photocatalyst, Methylene Blue, Niobium, Titania*

http://dx.doi.org/xx.xxx/xxx.xxx.xxx |

1. INTRODUCTION

Improper discharge from the textile industry causes contamination of water bodies [1]. It releases hazardous, mutagenic dyes, such as methylene blue, into the environment as pollutants [2]. Methylene blue is an aromatic organic dye with a deep blue color and is used in many real-life applications. Due to degradation by oxidizing agents, it reduces light transmission in water, leading to the death of aquatic organisms from a lack of sunlight. As the impacts on aquatic organisms intensify, a safe method for degrading this pollutant is urgently needed. Hence, various methods, such as Fenton's reagent [3], which can remove water-soluble and water-insoluble dyes, and ion exchange, were employed to degrade MB. However, it was insufficient because of the MB's recalcitrance. These limitations have led to the development of advanced oxidation processes (AOPs). AOPs are a promising technique for remediating contaminated industrial wastewater. It generates reactive species, such as (OH), that can degrade MB into low or non-toxic molecules [4].

Among the various AOP processes, photocatalysis is chosen because it can remove pollutants at ambient temperature and pressure via oxidation [5,6], with the added advantage that it does not form secondary pollutants that can harm water bodies [7]. The efficiency depends on the semiconductor catalyst used, with titanium dioxide among the materials investigated [8]. It is a valuable catalyst with high performance, owing to its inertness, non-toxicity, and affordability. However, the performance is disrupted by the high bandgap and agglomeration of titania, which reduces catalytic activity. This is coupled with the problem of a fast recombination rate between electron and hole [9].

To improve its photocatalytic performance, titania can be modified through metal doping. Niobium, one of the pentavalent elements, has been reported as an effective dopant to decrease the bandgap of titania [10]. Niobium dopants introduce impurities into the titania structure by acting as electron donors. It can delay electron-hole recombination and enhance photocatalytic properties.

Nevertheless, the photocatalyst's performance remains poor because the mixture readily forms agglomerates [11]. To overcome this, the literature indicates the need to provide support to disperse pollutants onto the photocatalyst [12] and to enhance the photocatalysis process.

Mesoporous fumed silica is a promising support material due to its high surface area and good structural stability [13]. Mesoporous fumed silica exhibits a surface area of 90 to 140 m^2/g, which can be further increased by additional treatment [14]. The loading of fumed silica is applied to disperse the titania particles and prevent agglomeration. This enhances the photocatalyst's catalytic behaviour in degrading methylene blue by providing sufficient diffusion area for methylene blue adsorption and initiating the degradation process.

In this study, mesoporous silica-supported niobium-doped titanium dioxide was synthesized by using the sol-gel method. The synthesized photocatalysts were characterized to evaluate their physicochemical properties. The photocatalytic activity of the prepared photocatalyst was investigated for the degradation of methylene blue under visible light irradiation. In addition, the synergistic effect of silica support with niobium-doped TiO_2 was examined, while the influence of methylene blue concentration was studied to determine the optimal conditions for the photocatalytic process.

2. EXPERIMENTS

2.1 Preparation of niobium precursor solution

The niobium precursor solution was prepared by dissolving 0.23 g of ammonium niobate(V) oxalate hydrate in distilled water. Then it was stirred until a homogeneous solution was obtained. All of these methods are adapted from the research done [8].

2.2 Synthesis of TiO_2 and 5% niobium-doped TiO_2

2 mL of TTIP solution and 7.5 mL of 2-propanol were mixed inside a pre-heated beaker. Then, the mixture was stirred constantly for 15 minutes while heating it to 70°C. When the temperature reached 70°C, 0.6 mL of acetic acid was added, and the mixture was swirled for 15 minutes. It was further added with ethylene glycol while stirring for 10 minutes. The mixture was aged for 24 hours and dried at 70°C for 12 hours. Lastly, it was ground and calcined at 450°C for 4 hours overnight.

The method was the same as for the synthesis of TiO2, with the addition of the niobium precursor solution, followed by stirring for 23 minutes. Then, the mixture was aged, dried, and calcined.

2.3 Synthesis of mesoporous silica-supported niobium-doped TiO_2

2 mL of TTIP solution and 7.5 mL of 2-propanol were mixed inside a pre-heated beaker. Then, the mixture was stirred constantly for 15 minutes while heating it to 70°C. When the temperature reached 70°C, 0.6 mL of acetic acid was added, and the mixture was swirled for 15 minutes. It was further added with ethylene glycol while stirring for 10 minutes. Next, the niobium precursor solution was added while stirring for 23 minutes. Then, different weights of fumed silica were alternately added to 20 mL of distilled water to synthesize SiO_2/Nb-TiO_2 at 10, 20, and 30. After all fumed silica had been added, the mixture was sonicated first for 20 minutes before being aged for 24 hours. Then, it was dried at 70°C for 12 hours. Lastly, the sample was ground and calcined at 450°C for 4 hours overnight.

2.4 Characterization

The phase purity of the prepared photocatalysts was evaluated using X-ray diffraction (XRD). The optical absorbance was measured by diffuse reflectance UV-Visible spectroscopy (DRUV-Vis), and porosity was assessed by nitrogen adsorption-desorption analysis. The chemical functional group of the photocatalyst was measured using Fourier transform infrared-attenuated total reflection spectroscopy (FTIR-ATR).

2.5 Photocatalytic degradation of MB

The photocatalytic performance of the prepared photocatalysts was evaluated by measuring the photodegradation of methylene blue under visible light irradiation. The photocatalytic degradation of methylene blue solution was performed using a simple reactor model equipped with a visible-light irradiation source using a 15 W LED lamp with a UV cut-off filter ($\lambda > 420$ nm). Photodegradation was carried out by stirring the solution in the dark for 30 minutes to reach equilibrium. Then, it was exposed to visible light for 120 minutes. Every 30 minutes, absorbance was measured using a PerkinElmer Lambda 35 UV-Visible Spectrophotometer.

3. RESULTS AND DISCUSSION

3.1 Characterization of photocatalysts

In this study, XRD analysis was conducted on the representative silica-supported samples, 20 SiO_2/Nb-TiO_2, Nb-doped TiO_2, and TiO_2, to evaluate the phase composition. According to Figure 1, the undoped TiO_2 peaks were observed at $2\theta = 25.44°$ (101), 37.91° (004), and 48.23° (200), which were attributed to anatase TiO_2. It aligned with the JCPDS 84-1286 [3]. Niobium was successfully incorporated into the crystal structure of titania by shifting to a lower 2θ value of 25.31° from 25.44°. The lattice expansion occurred because Nb^{5+} substituted for Ti^{4+} ions, and localized strain was formed, thereby reducing the oxygen vacancy concentration [15]. This is crucial because excess oxygen vacancies can act as a recombination centre. The substitution also prevented the formation of the rutile

phase [3].

For 20 SiO_2/Nb-TiO_2, the broad hump at 25.47° without a sharp peak confirmed attribution to a pure amorphous material. As a representative sample with silica modification, the 20 SiO_2/Nb–TiO_2 sample was characterized by XRD to investigate the structural effects of silica incorporation on the crystalline phase of TiO_2. With silica loading as the only variable parameter, all samples were synthesized and calcined under identical conditions, resulting in similar diffraction characteristics of anatase TiO_2 [12]. Therefore, adsorption behavior and surface properties are more likely to explain variances in photocatalytic performance than major crystallographic modifications.

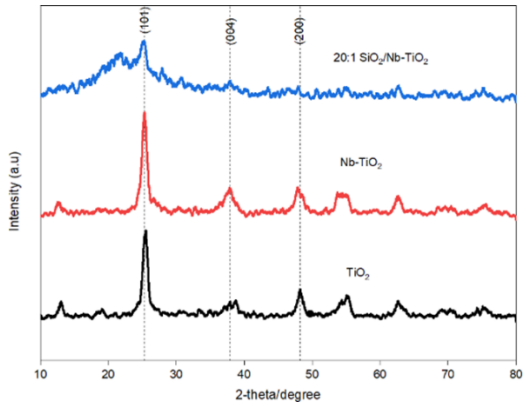

Figure 1. XRD diffractograms of undoped TiO_2, niobium-doped titania and 20 SiO_2/Nb-TiO_2

Figure 2 displays the FTIR-ATR spectra of pure titania, niobium-doped titania, and silica-to-titania ratios of 10, 20, and 30 SiO_2/Nb-TiO_2. The FTIR spectra of TiO_2 and niobium-doped TiO_2 were broad and well defined, centered at 3267 cm^{-1}. On the other hand, all silica-supported samples exhibited a poorly defined, low-intensity, broad absorption centered at the same wavelength, which is attributed to the stretching vibration of hydroxyl groups (O–H) and indicates the presence of Brønsted acid sites [16]. The intensity of the band in titania and Nb-doped TiO_2 was higher than in silica-supported samples, suggesting a higher surface hydroxyl density. A high density of surface OH groups promoted surface hydroxylation. It generated more hydroxyl radicals during methylene blue degradation.

Niobium oxide doping reduced the O-H intensity, consistent with an increase in the acidic character of the titania lattice. It significantly altered the metal-oxygen bonding and reduced organic residues in the FTIR-ATR spectra [17]. The Ti-O vibration was observed at 687 cm^{-1} [8]. For silica-supported niobium-doped titania, a broad band centered at 1062 cm^{-1} confirmed the unsymmetric stretching of the Si-O-Si bond. The peaks at 803 cm^{-1} and 796 cm^{-1} were assigned to the bridging oxygen between Nb bonds and to symmetric stretching of the Si-O-Si network. The modification of the Si-O-Si and Ti-O vibration bands in the ATR-FTIR analysis suggested strong interfacial interactions between Nb-TiO_2 and the silica support.

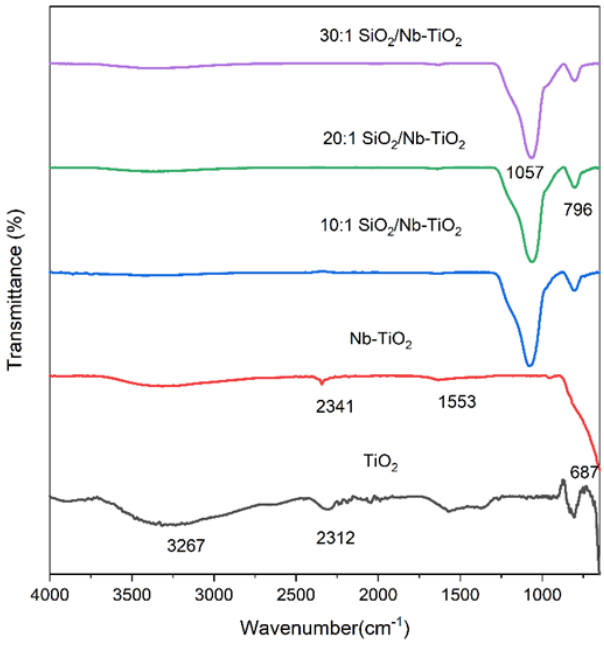

Figure 2. FTIR-ATR spectra of pure titania, niobium-doped titania, and all silica-supported niobium-doped titania

The optical band gaps of the prepared materials were evaluated through the Tauc plot in Figure 3. The bandgap of the TiO_2, Nb-TiO_2, 10, and 20 SiO_2/Nb-TiO_2 are 3.33, 3.26, 3.49, and 3.60 eV, respectively. It was observed that the bandgap energy of all silica-supported samples was higher than that of titania and niobium-doped titania. This increment was attributed to the quantum-size effect and to improved dispersion of TiO_2 particles on the silica surface [16]. Nevertheless, the bandgap of all silica-supported samples was significantly reduced, as the bandgap of amorphous silica is around 3.8 eV [18]. There was a decrease in bandgap for niobium-doped titania compared to pure titania, which was 3.33 eV. This was due to the successful doping of niobium into TiO_2. The niobium dopant, as a pentavalent element, was able to generate a temporary energy level between the valence band (VB) and conduction band (CB) of TiO_2 [3].

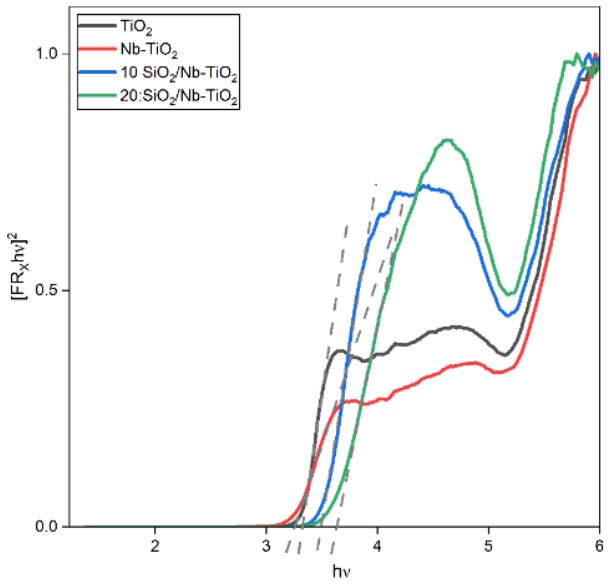

Figure 3. Graphs of $[FR_X h\upsilon]^2$ against hυ using the Tauc equation and Kubelka-Munk equation

All prepared materials in Figure 4 showed a peak of around 215 nm. It is correlated to the charge transfer of isolated tetrahedral titanium species [19], while the range of absorption around 260-320 nm is related to octahedral titanium species. Titania and niobium-doped TiO_2 absorption edges were found at 330 nm and exhibited strong absorption in the UV region due to the intrinsic interaction of electrons when they jump from the VB band to the CB [3]. The Nb-TiO_2 showed a slight red-shift absorption edge compared to TiO_2. This suggested a narrowing of the bandgap due to niobium substitution and lattice distortion.

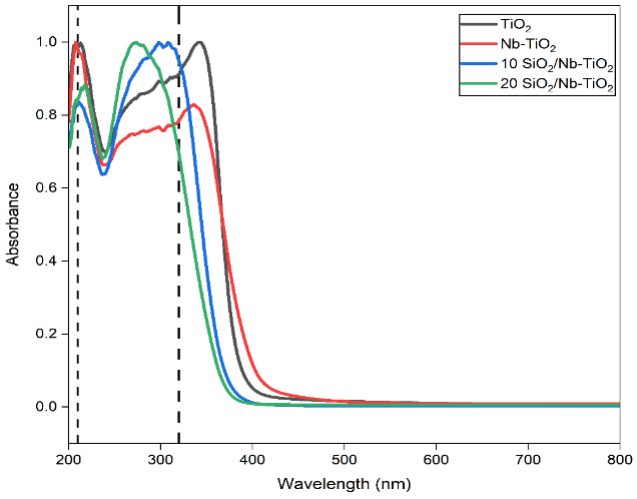

Figure 4. UV-vis diffuse reflectance spectra of the prepared samples.

Based on the IUPAC classification [20], all the prepared samples tabulated in Table 1 fell within the mesoporous range because the pore diameter was in the range between 2 and 50 nm. The Brunauer-Emmett-Teller (BET) method was used to calculate surface area.

Table 1. Surface area, pore volume, and average pore size of TiO_2, Nb-TiO_2, and 10 SiO_2/Nb-TiO_2

Samples	Surface Area (m^2/g)	Average pore size (nm)
TiO_2	45.86	8.02
Nb-TiO_2	71.71	6.13
10 SiO_2/Nb-TiO_2	180.81	28.78

The synthesized titania in Figure 5 displays a type IV isotherm with H2 hysteresis loop. It was a product of an interconnected effect [21]. Meanwhile, Nb-doped TiO_2 and 10 SiO_2/Nb-TiO_2 exhibited a type IV isotherm with H3 hysteresis loop that possessed slit-shaped pores. 10 SiO_2/Nb-TiO_2 sample exhibited the highest surface area, which was 180.81 m^2/g, compared to Nb-doped TiO_2 and TiO_2.This shows that fumed silica successfully acted as a support, preventing titania agglomeration. Nb-doped TiO_2 had a higher surface area than TiO_2 due to a lower crystallite size [22]. Hence, the high surface area of the silica-supported sample can increase the number of redox reaction sites, leading to a higher percentage of MB degradation [8].

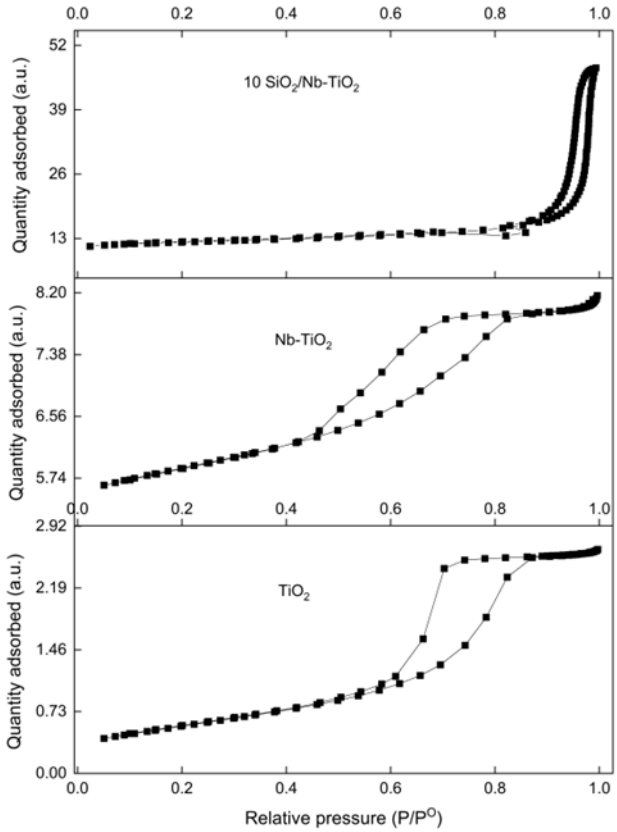

Figure 5. Adsorption-desorption isotherms of TiO_2, Nb-TiO_2 and 10 SiO_2/Nb-TiO_2

3.2 Photocatalytic degradation of MB

The photodegradation of methylene blue (MB) under visible light was used to determine the photocatalytic activity of SiO_2/Nb-TiO_2. The degradation efficiencies of photocatalyst TiO_2, Nb-TiO_2, 10, 20, and 30 SiO_2/Nb-TiO_2 when degrading 10 ppm MB is 7.11%, 3.19%, 5.36%, 82.68%, and 15.25%. respectively. As depicted in Figure 6, all silica-supported samples have higher catalytic degradation than TiO_2 and Nb-TiO_2. The photocatalytic degradation efficiency of all prepared materials increased with longer irradiation times. This suggested that the reaction species were continuously produced during the process. The highest degradation activity was performed by 20 SiO_2/Nb-TiO_2, which had a suitable silica-to-titania ratio to prevent titania agglomeration. The lowest degradation activity was performed by Nb-doped TiO_2.

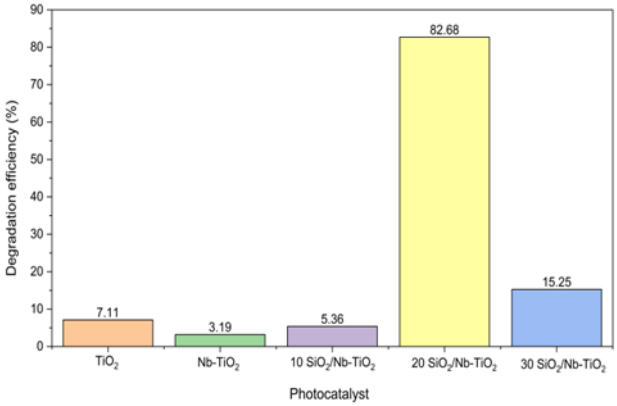

Figure 6. Photocatalytic degradation efficiency of 10 ppm methylene blue versus irradiation time of TiO_2, niobium-doped TiO_2, and all silica-supported samples under visible light irradiation for 2 hours. (Reaction conditions: MB 10 ppm)

However, the degradation efficiency results showed little distribution and consistency across the prepared materials. The least amount of methylene blue was degraded by the niobium-doped TiO_2 photocatalyst. This slightly contradicts Cheema's study [17], which showed that the niobium-doped sample exhibited higher photocatalytic degradation than titania. To further investigate the effect of dye concentration, photocatalytic degradation efficiency was measured at a lower MB concentration, 5 ppm, under identical conditions.

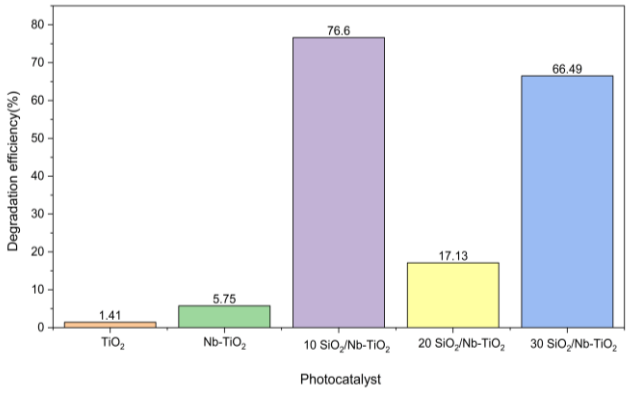

Figure 7. Photocatalytic degradation efficiency of 5 ppm methylene blue versus irradiation time, TiO_2, niobium-doped TiO_2, and all silica-supported samples under visible light irradiation for 2 hours. (Reaction conditions: MB 5 ppm)

The results of a 120-minute investigation of the synthesized sample's photocatalytic activity in the breakdown of 5 ppm MB are shown in Figure 7. Evidently, 10 SiO_2/Nb-TiO_2 degraded at the highest (76.60%),

followed by 30 SiO_2/Nb-TiO_2 (66.49%), 20 SiO_2/Nb-TiO_2 (17.13%), Nb-TiO_2 (5.75%), and TiO_2 (1.41%). Compared to pure TiO_2 and Nb-doped TiO_2, 10 SiO_2/Nb-TiO_2 showed higher activity. This performance was attributed to reduced light attenuation in the solution and to a greater number of photons reaching the photocatalyst, thereby driving the reaction and degradation [23]. Although the measured band gap values remain within the UV-responsive region, Nb doping of TiO_2 can introduce defect states and increase charge transfer under visible light, thereby broadening the absorption range and accelerating electron-hole pair separation [24]. As a result of defect engineering, oxygen vacancies can be generated at the surfaces of dopant ions, thereby increasing the quantum efficiency of the system and, in turn, its photocatalytic activity [25].

A photocatalytic model was tested under different pollutant loading conditions using methylene blue concentrations of 5 and 10 ppm. The difference in the optimal silica-to-titania ratio across methylene blue concentrations indicated that adsorption capacity and light penetration influence photocatalyst performance. At high MB dye concentration (10 ppm), adsorption became a limiting factor for the photodegradation rate. The 5 ppm solution provides relatively dilute conditions with minimal light attenuation, while the 10 ppm solution presents a more challenging environment with a higher dye concentration, reduced photon penetration, and increased competition for active sites. Silica ratios that were too high or too low could reduce the degradation rate [11]. A high silica content exposed less titania to light, reducing the degradation rate. At high silica content, the titania active site was covered by silica, resulting in poor degradation efficiency [26]. Meanwhile, a dye concentration of 5 ppm reduced the titania surface saturation due to the low volume of the silica support. Many MB dyes can adsorb to the titania surface. It was found that 10 SiO_2/Nb–TiO_2 exhibited the highest BET surface area; however, the photocatalytic performance at higher concentrations of methylene blue (10 ppm) may be affected by excessive dye adsorption, partial blockage of active sites, and reduced light penetration due to increased coloration of the dye solution [27]. Hence, surface area alone does not determine photocatalytic efficiency under higher pollutant loading conditions. Therefore, the photocatalytic performance may vary depending on the interplay among adsorption behavior, surface properties, and light-utilization efficiency.

4. CONCLUSION

This study successfully synthesized mesoporous silica-supported niobium-doped titania using the sol-gel method. It also successfully evaluated the catalytic performance of the prepared materials as photocatalysts under visible light. by examining the materials using XRD, FTIR-ATR, DRUV-Vis, and N_2 Adsorption-Desorption analysis. Overall, the fumed silica appears to be an attractive support for niobium-doped titania, improving photocatalytic degradation performance. It is observed that 10 SiO_2/Nb-TiO_2 is the best photocatalyst for the degradation of methylene blue under visible light, achieving the highest degradation percentage compared to pure TiO_2 and Nb-TiO_2, and exhibiting the highest surface area and the lowest band gap. To conclude, 10 SiO_2/Nb-TiO_2 demonstrated the best performance for MB degradation under visible light due to the beneficial synergistic effect of silica support and niobium oxide doping.

ACKNOWLEDGEMENTS

The authors would like to acknowledge the financial support obtained from the Ministry of Higher Education Malaysia (MOHE) and Universiti Teknologi Malaysia (UTM) through the Potential Academic Staff grant (Cost centre: QJ130000.2754.03K86).

REFERENCES

[1] Himanshi, Jasrotia, R., Grover, A., Somvanshi, A., Wahab, S., Almoyad, M. A. A., Suman, Katoch, G., & Rai, R. (2025). Advances in magnesium spinel ferrites for photocatalytic degradation of methylene blue: Challenges and future prospectives. Journal of Magnesium and Alloys.

[2] Al-Tohamy, R., Ali, S. S., Li, F., Okasha, K. M., Mahmoud, Y. A. G., Elsamahy, T., Jiao, H., Fu, Y., & Sun, J. (2022). A critical review on the treatment of dye-containing wastewater: Ecotoxicological and health concerns of textile dyes and possible remediation approaches for environmental safety. Ecotoxicology and Environmental Safety, 231, Article 113160.

[3] Shili, B., Khaldi, O., Mendes-Felipe, C., Rosales, M., Alves, D. C., Martins, P. M., Ben Younes, R., & Lanceros-Mendez, S. (2025). Synthesis of Nb-Doped TiO_2 Nanoparticles for Photocatalytic Degradation of Ciprofloxacin: A Combined Experimental and DFT Approach. Nanomaterials, 15(17), 1307.

[4] Liau, L. S., Ling, C. M., Ha, S. T., Attan, N., & Lee, S. L. (2025). Technische Universiteit Delft-1-supported nickel oxide-doped titanium dioxide for oxidative removal of methylene blue. Malaysian Journal of Analytical Sciences, 29(4), Article 1538.

[5] de Moraes, N. P., et al. (2023). "Using KNbO3 catalyst produced from a simple solid-state synthesis method in a new piezophotocatalytic ozonation hybrid process." Ceramics International 49(18): 30090-30103.

[6] Al Miad, A., Saikat, S. P., Alam, M. K., Sahadat Hossain, M., Bahadur, N. M., & Ahmed, S. (2024). Metal oxide-based photocatalysts for the efficient degradation of organic pollutants for a sustainable environment: a review. Nanoscale Advances, 6(19), 4781-4803.

[7] Singh, P., Abdullah, M. M., Ahmed, M., & Ikram, S. (2019). Photocatalysis: perspective, mechanism, and applications. Nova Science.

[8] Awais, M., Khursheed, S., Tehreem, R., Mok, Y. S., & Siddiqui, G. U. (2022). pH-regulated rapid photocatalytic degradation of methylene blue dye via niobium-nitrogen co-doped titanium dioxide nanostructures under sunlight. Applied Catalysis A:General,643,118764.

[9] Ling, C. M., Ong, S.-T., & Lee, S. L. (2025). Recent development of surface-modified titanium dioxide for enhanced oxidation catalytic activity: A short review. Journal of Alloys and Compounds, 1037,182226.

[10] Paul, R., Das, A., Sharma, N., Choudhury, S. P., & Parthiban, S. (2026). The origin of enhanced photocatalytic performance in titanium dioxide via niobium doping: From experimental assessments to DFT insights. Colloids and Surfaces A: Physicochemical and Engineering Aspects, 728, 138830.
[11] Ulfa, M., Anggreani, C. N., & Sholeha, N. A. (2023). Fine-tuning mesoporous silica properties by a dual-template ratio as TiO2 support for dye photodegradation booster. Heliyon, 9(6), Article e16275.
[12] Ling, C. M., Yuliati, L., Lintang, H. O., & Lee, S. L. (2020). TUD-C-supported tungsten oxide-doped titania catalysts for cyclohexane oxidation. Malaysian Journal of Chemistry, 22(2), 29-36.
[13] Afzal, S., Hassan, S., Alahmadi, A. N. M., Masud, M. I., Imran, Z., Karamat, S., & Kashif, M. (2026). Heterogeneous electron-driven photocatalytic degradation of methylene blue dye using heterojunction SiO2/MoO3 electrospun nanofibers: Synthesis, characterizations and application. Journal of Water Process Engineering, 81,109360.
[14] Li, Q., Ouyang, H., Yang, X., Wang, Q., Ding, Y., Yu, H., & Rao, Z. (2025). Synthesis, characterization, and photophysical properties of europium complex-functionalized fumed silica and its corresponding PMMA-doped composites. RSC Advances, 15(32), 25885-25893.
[15] Zeng, C., et al. (2024). "Revisiting the crucial roles of oxygen vacancies in photo/electro-catalytic degradation of aqueous organic pollutants." Applied Catalysis O: Open 190: 206930.
[16] Babyszko, A., Wanag, A., Sadłowski, M., Kusiak-Nejman, E., & Morawski, A. W. (2022). Synthesis and characterization of SiO_2/TiO2 as photocatalyst on methylene blue degradation. Catalysts, 12(11), 1372.
[17] Cheema, A. N., Muneer, I., Maham, Yasmeen, F., & Ali, D. (2025). Impact of niobium doping on photocatalytic degradation efficiency of iron oxide nanoparticles for methylene blue dye under UV and sunlight. Materials Science and Engineering: B,312,117878.
[18] Alibe, I., Matori, K., Saion, E., Alibe, A., Zaid, M., & Engku, E. (2016). A facile synthesis of amorphous silica nanoparticles by simple thermal treatment route. Dig J Nanomater Biostruct, 11(4), 1155-1164.
[19] Hatta, M. H. M., Matmin, J., Nur, H., & Batumalaie, K. (2021). Synthesis and Characterization of Titanium Catalyst Containing Polystyrene Composites for Epoxidation Of 1-Octene. Malaysian Journal of Catalysis, 5(1).
[20] Beltrán-Aburto, R., Borjas-García, S. E., Martínez-Torres, P., Villegas, J., & Medina Flores, A. (2025). Synthesis of Mesoporous Samarium Oxide by Using CTAB. Microscopy and Microanalysis, 31.
[21] Zhao, L., Sun, J., E., S., Sheng, K., Wang, K., Zhang, X., 2024. Synthesis and characterization of TiO_2/ hydrochar matrix composites for enhanced ammonia degradation. RSC Advances 14, 12131–12141.
[22] da Silva, A. L., Hotza, D., & Castro, R. H. R. (2017). Surface energy effects on the stability of anatase and rutile nanocrystals: A predictive diagram for Nb2O5-doped-TiO2. Applied Surface Science,393,103109.
[23] Oladoye, P. O., Ajiboye, T. O., Omotola, E. O., & Oyewola, O. J. (2022). Methylene blue dye: Toxicity and potential elimination technology from wastewater. Results in Engineering, 16, 100678.
[24] Acharya, R., & Pani, P. (2022). Visible light susceptible doped TiO2 photocatalytic systems: An overview. Materials Today: Proceedings, 67, 1276-1282.
[25] Ferreira, M. P., & Carvalho, H. B. d. (2022). On the processing of anatase La-doped TiO2 nanopowders: structural phase transition and surface defect engineering. Condensed Matter-Materials Science, 1-18.
[26] Saeedi, S. N., Rasoulifard, M. H., Dorraji, M. S. S., Douroudgari, H., & Sehati, N. (2025). Enhanced photocatalytic degradation of organic pollutants using a TiO(2)-clay nanocomposite in a rotary photoreactor with experimental and theoretical insights. Sci Rep, 15(1), 38193.
[27] Reza, K. M., Kurny, A., & Gulshan, F. (2017). Parameters affecting the photocatalytic degradation of dyes using TiO2: a review. Applied Water Science, 7, 1569-1578.